Mathematical and Computational Applications, Vol. 16, No. 2, pp. 456-466, 2011.

EVALUATION OF OPTIMAL SENSOR PLACEMENT TECHNIQUES FOR PARAMETER IDENTIFICATION IN BUILDINGS

Pelin GÜNDEŞ BAKIR
Department of Civil Engineering
Istanbul Technical University
İTÜ Ayazağa Kampüsü,Maslak, 34469, Istanbul, Turkey
gundes@itu.edu.tr, gundesbakir@yahoo.com

Abstract- This paper addresses the application of six different optimal sensor placement (OSP) techniques in buildings. These techniques are the EFfective Independence (EFI), Optimal Driving Point (ODP), Non-Optimal Driving Point (NODP), Effective Independence Driving Point Residue (EFI-DPR), Singular Value Decomposition (SVD) and the Sensor Set Expansion (SSE) methods. A toolbox OPTISEP is developed by the author for this purpose within the context of this paper. The techniques are compared among themselves by using various criteria. The overall results show that the SSE Technique is the best. First, the technique results in a dramatic reduction in the computational effort. Second, it allows a civil engineer to specify a set of locations that they absolutely want to keep in the final sensor configuration. Mozst importantly, while the sensor distribution estimated by other techniques is mainly concentrated in a certain storey of the building, SSE gives a homogeneous sensor distribution throughout the building. Finally, it is shown that the technique is also robust against noise in the measurements.
Key Words- Optimal sensor placement, Fisher information matrix, multistory buildings, system identification, modal testing

1.INTRODUCTION

The sensor location problem is a key issue for on-orbit modal identification and correlation of large space structures (LSS) in aerospace industry. The Optimal Sensor Placement (OSP) techniques are discussed comprehensively for aerospace applications [1,2,3], for process industry [4], for the safe operation of nuclear reactors [5] and for bridges [6,7].

This paper addresses the application of different OSP techniques in stiff buildings. As stated above, the OSP Techniques were first developed for aerospace structures where the stiffness and the mass distributions are homogeneous throughout the structure. However, in reinforced concrete buildings, the stiffness and the mass distributions are not homogeneous [8,9]. Therefore, it is very important to investigate the feasibility of these techniques in the application for building type structures.

A TUBITAK project entitled 'Damage identification in existing buildings using real time system identification techniques and finite element (FE) model updating' has been started in 2008 at Istanbul, Turkey. Within this paper as well as the context of the project, a toolbox OPTISEP (OPTImal SEnsor Placement) is developed in MATLAB [10] by the author which can compute the optimum sensor locations according to six alternative OSP techniques currently used in NASA for LSS. Different techniques that are incorporated in the toolbox are the EFfective Independence (EFI) by Kammer [1], Optimal Driving Point (ODP) [11,12], Non-Optimal Driving Point (NODP) [11],

Effective Independence-Driving Point Residue (EFI-DPR) [11,19], the Singular Value Decomposition based technique (SVD-OSP) by Kim et al. [13] and the Sensor Set Expansion (SSE) by Kammer et al. [14]. The optimal sensor locations for a stiff building are determined based on the different OSP techniques in the toolbox and are compared with each other using various criteria in this paper.

2 .OPTIMAL SENSOR PLACEMENT TECHNIQUES

2.1 The Effective Independence Method (EFI)

The EFI Method by Kammer [1] is used for the selection of a set of sensor locations from a large set for the purpose of on-orbit identification and correlation of LSS [15]. If the sensor output equation is as:

$$\mathbf{u}_s = \Phi_s \mathbf{q} \tag{1}$$

the sensors can be sampled and an estimate can be calculated for the target states $\hat{\mathbf{q}}$ by solving Eq.(1) as:

$$\hat{\mathbf{q}} = [\Phi_s^T \Phi_s]^{-1} \Phi_s^T \mathbf{u}_s \tag{2}$$

where $\mathbf{u}_s$ is the output from the sensors, Φ_s the matrix of the target modes partitioned to the sensor locations obtained from the FE model, and $\mathbf{q}$ is the vector of target modal coordinates. The best estimate in placing m sensors within the s candidate locations implies that the covariance matrix of the estimate errors will be a minimum. Within this context, the output $\mathbf{u}_s$ must be modified as:

$$\mathbf{u}_s = H(\mathbf{q}) + N = \Phi_s \mathbf{q} + N \tag{3}$$

where H is the process measurement and the vector N represents the stationary Gaussian white noise with variance Ψ_o^2. The covariance matrix of the estimate error can be expressed as:

$$P = \boldsymbol{E}[(q-\hat{q})(q-\hat{q})^T] = \left[\left(\frac{\delta H}{\delta q}\right)^T [\Psi_o^2]^{-1} \left(\frac{\delta H}{\delta q}\right)\right]^{-1} \tag{4}$$

where $\boldsymbol{E}$ denotes the expected value. Since $H(\mathbf{q}) = \Phi_s \mathbf{q}$, the covariance matrix can be simplified as:

$$P = \left[\Phi_s{}^T (\Psi_o{}^2)^{-1} \Phi_s\right]^{-1} = Q^{-1} \tag{5}$$

where Q is the Fisher Information Matrix (FIM) [16]. The best state estimate $\hat{\mathbf{q}}$ can be obtained by maximizing Q which results in the minimization of the covariance matrix. It is assumed that the measurement noise is identically and independently distributed random process at each sensor. The FIM can then be simplified from Eq.(5) as [1]:

$$Q = \frac{1}{\Psi_o{}^2} \Phi_s{}^T \Phi_s = \frac{1}{\Psi_o{}^2} A_o \tag{6}$$

The following eigenvalue problem is solved:

$$[A_o - \lambda I]\Psi = 0 \tag{7}$$

The eigenvalues of A_o are real and positive and the eigenvectors Ψ are orthonormal resulting in the relations:

$$\Psi^T \mathbf{A}_o \Psi = \lambda \qquad \Psi^T \Psi = \mathbf{I} \tag{8}$$

The derivation of the fractional eigenvalue F_E distribution is given elsewhere [1,15]. The independence distribution vector E_D can be expressed as the diagonal of the matrix E :

$$E = \Phi_s \Psi \lambda^{-1} \Psi^T \Phi_s{}^T = \Phi_s A_O^{-1} \Phi_s{}^T \tag{9}$$

E can then be expressed as:

$$E = \Phi_s [\Phi_s{}^T \Phi_s]^{-1} \Phi_s{}^T \tag{10}$$

The diagonal element that has the smallest value in the prediction matrix represents the degree of freedom and the corresponding sensor that has the smallest contribution to the identification of Φ_s. This sensor location can be eliminated from the initial set of candidate sensors in an iterative way until the number of sensors in the initial candidate set equals the fixed sensor number *m* being used.

2.2 Optimum Driving Point (ODP) Based Method

In order to identify the nodal points of mode shapes, modal constants for all chosen modes at each degree of freedom are multiplied and the result is a coefficient called the ODP parameter which can be expressed as:

$$ODP(i) = \prod_{r=1}^{k} \| \phi_{i,r} \| \tag{11}$$

The candidate sensor locations are reduced to the number of available sensors using the ODP parameter. The sensor locations with the low ODP values are deleted first.

2.3 Non-Optimum driving point (NODP) based method

This methods uses the NODP parameter technique which for each DOF within a specified frequency range, identifies how close that DOF is to a nodal line of any mode. The technique evaluates the optimum driving positions as:

$$NODP(i) = \min_{r} (\| \phi_{i,r} \|) \tag{12}$$

2.4 The Effective Independence-Driving Point Residue Method (EFI-DPR)

In EFI-DPR methods [11,19], the $ADDOFV(i)$ of all DOF is accounted such that the DOFs with low response are deleted first. The EFI-DPR is defined below:

$$E_{ii}^{EFI-DPR} = E_{ii} ADDOFV(i) \tag{13}$$

where

$$ADDOFV(j) = \sum_{r=1}^{k} \frac{\Phi_{jr}^2}{\omega_r} \tag{14}$$

where ω_r is the *r*th target mode frequency.

2.5 Singular Value Decomposition Based Method (SVD-OSP)

A Singular Value Decomposition (SVD) based method is proposed by Kim and Park [13]. The details are in Ref [13] and will not be given here for purposes of brevity.

2.6 Sensor Set Expansion Technique

The SSE technique by Kammer [14] iteratively expands an initial set of sensors to the desired number of sensors as opposed to the previous techniques, which reduce the initial candidate set of sensors to the available number of sensors. The method allows a test engineer to specify a set of locations that they absolutely want to keep in the final sensor configuration. The techniques mentioned previously in this paper do not

retain certain locations in the final sensor configuration. There are two different cases when using the technique by Kammer [14]. The case in which the initial node set renders target mode shapes linearly independent is explained in the Appendix. If the initial node set renders target mode shapes linearly dependent, the FIM becomes singular with rank $l < k$. Let Q_o be the FIM that corresponds to the initially selected set of triaxes, ψ_o be the set of orthonormal eigenvectors associated with the zero eigenvalues of Q_o which span the $k-l$ dimensional space and which are orthogonal to the information subspace contained in Q_o. The eigenvectors ψ_o can be used to generate a corresponding orthogonal projector P that can be expressed as:

$$P = \psi_o \psi_o^T \tag{15}$$

The candidate sensor set information matrix Q_c can then be filtered using the relation:

$$\bar{Q}_c = P Q_c P^T \tag{16}$$

It should be noted that while Q_c is full rank, the projected information matrix $\bar{Q}_c$ is singular with rank $k-l$. This matrix can be decomposed as:

$$\bar{Q}_c = \bar{\psi} \bar{\lambda} \bar{\psi}^T \tag{17}$$

where $\bar{\psi}$ represents the orthonormal eigenvectors associated with the diagonal $k-l$ dimensional matrix $\bar{\lambda}$ containing the nonzero eigenvalues. The objective in the sensor set expansion technique is to remove the highest ranked node that contributes to $\bar{Q}_c$ from the candidate set and add it to the initial sensor set. The filtered candidate information matrix with the *i*th deleted candidate node can be written as:

$$\bar{Q}_{ai} = \bar{Q}_c - \bar{\phi}_{ai}^T \bar{\phi}_{ai} = \bar{\psi} \bar{\lambda} \bar{\psi}^T - \bar{\phi}_{ai}^T \bar{\phi}_{ai} \tag{18}$$

in which

$$\bar{\phi}_{ai} = \phi_{ai} P \tag{19}$$

The filtered candidate sensor set information matrix with the *i*th deleted candidate node can be decomposed as:

$$\bar{Q}_{ai} = \bar{\eta} \bar{\lambda}^{ai} \bar{\eta}^T \tag{20}$$

where $\bar{\lambda}^{ai}$ and $\bar{\eta}$ are the nonzero eigenvalues and the corresponding eigenvectors of $\bar{Q}_{ai}$. The measure of the triaxial EFI used to delete a sensor from the candidate set and add it to the initial sensor set in the rank deficient case is as:

$$Efi3_i^+ = \frac{det(\bar{\lambda}) - det(\bar{\lambda}^{ai})}{det(\bar{\lambda})} \tag{21}$$

3 . THE INSTRUMENTED SCHOOL BUILDING AND THE CANDIDATE SENSOR LOCATIONS

Different OSP techniques are tested in a five storey stiff school building (Fig.1). The modal frequencies calculated using the FE model are given in Table 1.

Figure 1: The instrumented school building [18].

Only four global modes can be used in damage identification as shown in Table 1. A three DOF candidate sensor is selected at each intersection point of axes that are shown in Fig.1 which summed up as a total 675 DOF for the candidate sensors for the whole building. The goal is to to select the sensor locations that would give the best estimates of the 4 target modes out of the initial candidate set of 675 sensor locations.

Table 1: Modal frequencies calculated using the FE model.

Number	Frequency (Hz)	Mode type
1	2.62	First bending mode in the z direction
2	4.84	First bending mode in the x direction
3	5.90	First torsion mode
4	10.007	Second bending mode in the z direction
5-12	10.133	Local modes of the ground storey beams
13	14.262	Local mode of the slabs
14	14.294	Local mode of the slabs
15	14.324	Local mode of the slabs
16	14.602	Local mode of the slabs
17	15.693	Local mode of the slabs
18	15.754	Local mode of the slabs
19	15.873	Local mode of the slabs
20	15.953	Local mode of the slabs

4 THE COMPARISON OF THE OPTIMAL SENSOR PLACEMENT TECHNIQUES

The resulting sensor configurations are shown in Figs. 2 and 3. It is apparent that while the sensor distribution is concentrated in the roof or in a certain storey of the structure in the other techniques, the final sensor configuration is homogeneously distributed throughout the storeys in the SSE technique. This shows that the SSE is more suited for applications in buildings than the other techniques. The figures also show that the EFI and the SVD-OSP methods give exactly identical results for the optimal sensor configuration. This should be anticipated as these two methods are in fact identical. The improvement that the SVD-OSP method brings on the EFI method is a criterion for deleting more number of sensors at one iteration.

The goodness of the sensor configuration estimated by the different methods can be compared in terms of the trace, the determinant and the condition number of the FIM. The determinant of the FIM is a measure of information amount in measurements. The condition number of the FIM is a measure of the sensor configuration estimations's

robustness to model errors in the mode shapes obtained from the FE method representation of the structure. First, the fractional eigenvalue distribution is illustrated in a three dimensional plot as shown in Fig. 4. Each peak in the plot shows the fractional contribution of each sensor location to the corresponding eigenvalue of the FIM. The figure demonstrates clearly that the highest fractional eigenvalue contributions are observed at the higher degrees of freedom.

Fig.5 shows the determinant values of the FIM calculated using different OSP techniques. The results show that the best OSP techniques are the EFI, SVD-OSP and EFI-DPR. The sensor configurations obtained using these three methods give more information regarding the mode shapes compared to the ODP and NODP methods. The figure also shows that NODP method gives the worst sensor configuration. Fig.6 shows that the EFI techniques result in a sensor configuration possessing a smaller estimate error covariance matrix yielding better state estimates than the NODP technique as they have higher trace values.

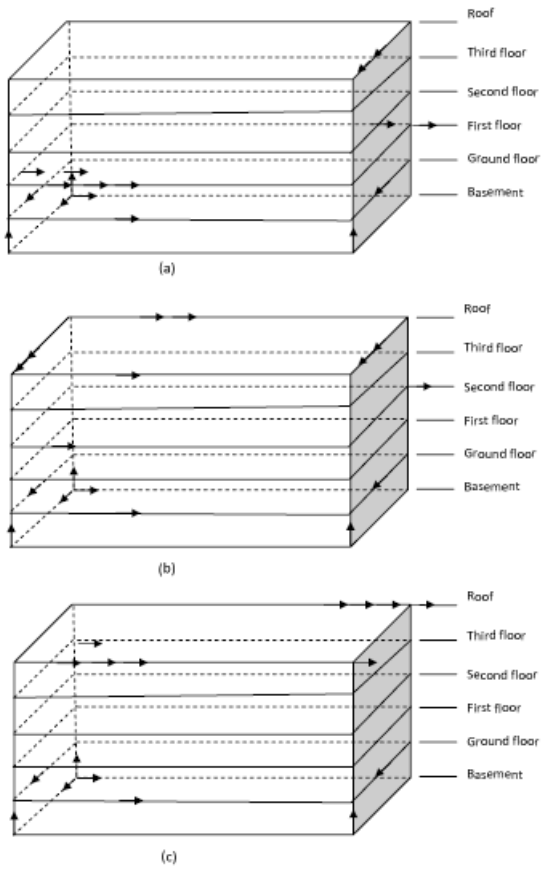

Figure 2: Final sensor configuration according to a) NODP (b) EFI and OSP-SVD (c)ODP method

The SSE technique could not be plotted in Figs. 5 and 6 together with the other techniques as the philosophy of the other techniques is the reduction of the sensor set rather than expansion of the initial subset of sensors. A comparison is made in Table 2 which clearly shows that the ODP and the NODP techniques should not be used in buildings due to dramatically low determinant values. Overall, the best result is obtained

from the SSE and the EFI techniques. However, if a choice has to be made between the EFI and SSE, SSE would always be preferable due to the fact that a more homogeneous sensor configuration is obtained with the SSE. Moreover, EFI tends to concentrate sensors at the roof level. The SSE technique also results in lower computation time than the EFI based techniques.

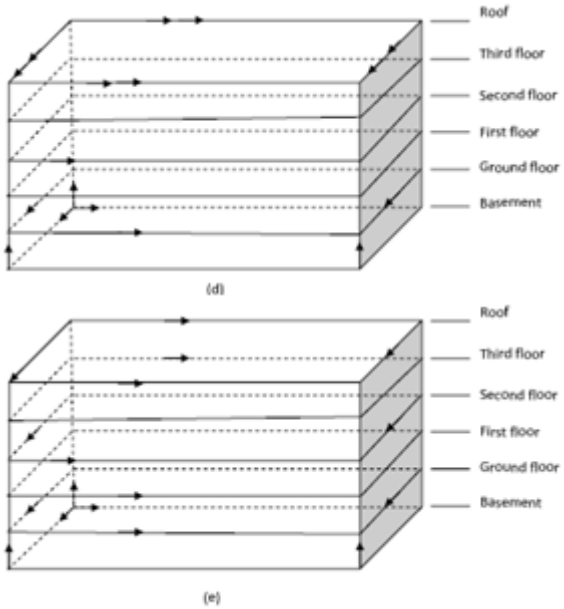

Figure 3: Final sensor configuration according to (d) EFI-DPR; (e) SSE

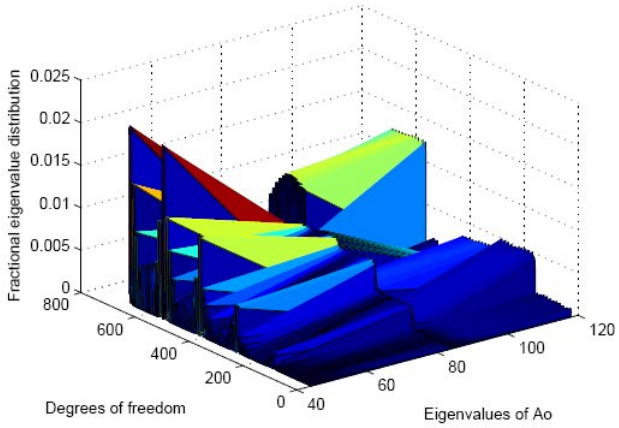

Figure 4: Fractional eigenvalue distribution for initial 675-DOF candidate sensor set and 4 target modes.

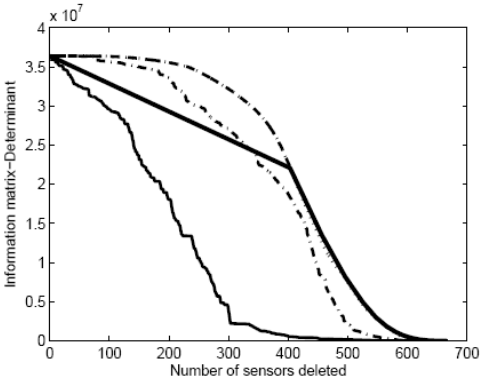

Figure 5: The Determinant of the FIM: NODP (solid line), EFI (dashed line), ODP (dashed-dotted line), EFI-DPR (dotted line) and the SVD-OSP methods (thick solid line).

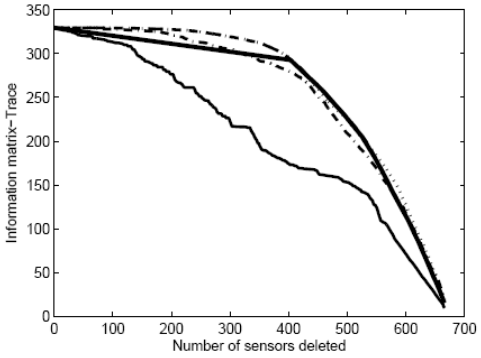

Figure 6: The Trace of the FIM: NODP(solid line), EFI (dashed line), ODP (dashed-dotted line), EFI-DPR (dotted line) and the SVD-OSP Methods (thick solid line).

Table 2: The condition number, the determinant and the trace obtained from different methods.

Technique	Condition Number	Trace	Determinant	CPU Time [sec]
NODP	7.61E6	4.7	1.9E− 12	2.094
EFI	2.5	9.9	29.09	2.087
ODP	7.8	10.68	1.2E-10	0.0823
EFI-DPR	6.7	11	22.15	2.24
SSE	3.89	10	30.1	0.05

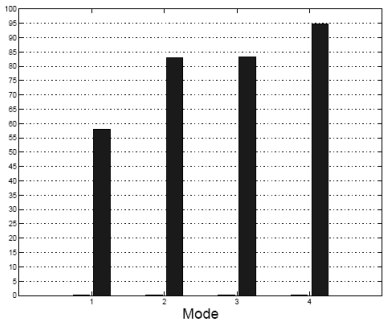

Figure 7: MAC values according to the NODP method.

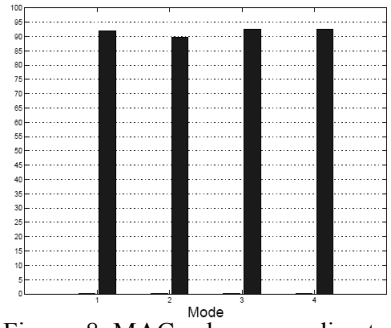

Figure 8: MAC values according to the EFI method.

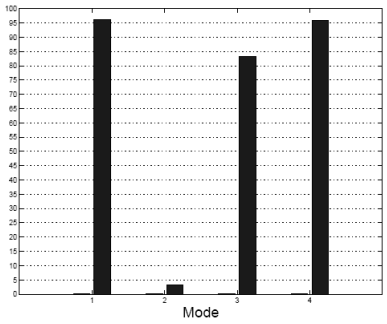

Figure 9: MAC values according to the ODP method.

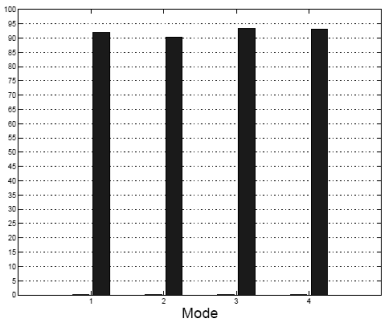

Figure 10: MAC values according to the EFI-DPR method.

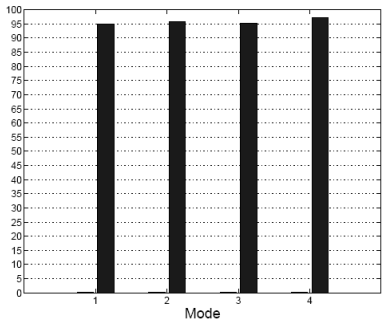

Figure 11: MAC values according to the SSE Technique.

Next, different OSP techniques are compared in terms of the Modal Assurance Criterion (MAC) values [17]. It should be noted that no system identification stage is involved in this study. This is an ongoing study. The effect of the sensor locations on the estimates of the system identification techniques is out of the scope of this paper and will be dealt with detail in another study. The aim in this paper is to investigate the robustness of each sensor placement technique to the presence of noise in the mode shapes. All the analytical modes obtained from the FE model are correlated with all the modes contaminated with noise and the results are placed in a matrix. In particular, the j^{th} component of the i^{th} mode contaminated with noise for the m^{th} measurement, ϕ_{ij}^{m}, is computed from the corresponding component of the same noise-free mode, ϕ_{ij} as:

$$\phi_{ij}^{m} = \phi_{ij} * \left(1 + \varsigma \zeta_i^m\right) \tag{22}$$

where ς is the standard deviation; and ζ_i^m is a random number in the range [-1,1]. The noise level is substantial in which ς is for the mode shapes. Figs. 7, 8,9, 10 and 11 show the MAC values based on an optimal sensor configuration determined by the NODP, EFI, ODP, EFI-DPR and the SSE Techniques, respectively. A MAC value below 95% is considered rather as unsatisfactory. These results show that overall, the SSE technique gives the best MAC values in the presence of substantial noise.

Only the diagonal terms of the MAC are considered in the above parametric studies. The off-diagonal terms are just as important. Ideally, they should be as small as possible. Fig. 12 shows that all the techniques except for the SSE have substantially high off-diagonal terms in their MAC. However, this is obviously not the case with the SSE method which shows the best capability in discriminating between different modes in the presence of substantially noisy measurements.

5. CONCLUSIONS

In this study, several different techniques developed for the OSP in LSS are implemented on multi-storey buildings. The overall results show that the SSE technique is the best and brings four important advantages over the other techniques: First, while the sensor configuration estimated by the other techniques is mainly concentrated at a certain floor of the structure, the SSE predicts a homogeneous sensor distribution throughout the structure. This would be very important in FE model updating as it is not

possible to know the location of the damage apriori in buildings. Second, the technique allows an expert civil engineer to keep a set of locations in the final sensor configuration. Third, the SSE technique decreases the computation time. Fourth, the technique is very robust against the noise in the measurements. Due to these advantages, the SSE method for on-orbit modal identification and correlation of LSS is promising and is well-suited for widespread use for sensor placement decision support in building type structures.

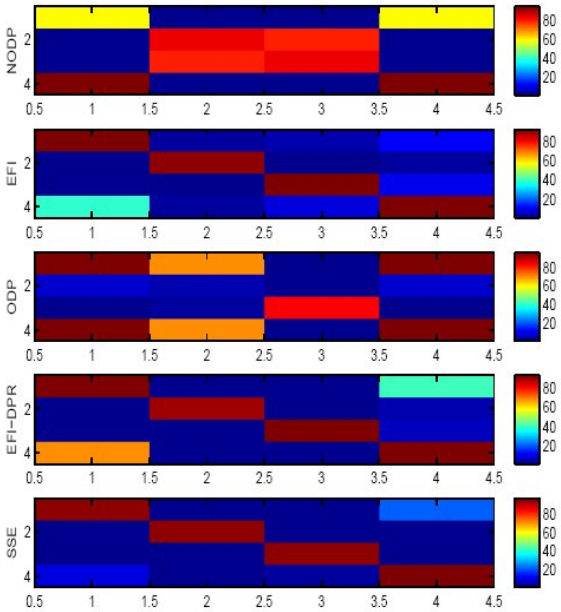

Figure 12: MAC Correlation matrix.

Acknowledgments- This study is carried out in the framework of the TUBITAK project 107M573 for which the author is the promotor. This financial support is acknowledged here.

6. REFERENCES

1 .Kammer D.C. Sensor placement for on-orbit modal identification and correlation of large space structures. *Journal of Guidance Control and Dynamics*, 14(2):251-59, 1991.
2. Kammer D.C. and Jensen B.M. and Mason D.R. Test-analysis correlation of the space shuttle solid rocket motor center segment. *Journal of Spacecraft and Rockets*, 26(4):266-73, 1989.
3. Kincaid R.K. and Padula S.L. D-optimal designs for sensor and actuator locations. *Computers and Operations Research*, 29(6):701-13, 2002.
4. Naimimohasses DM, Barnet DM and Smith PR. Sensor optimization using neural network sensitivity measures. *Measurement Science and Technology*, 6:1291-300, 1995.
5. Oh DY and No HC. Determination of the minimal number and optimal sensor location in a nuclear system with fixed incore detectors. *Nuclear Engineering and Design*, 152:197-212, 1994.
6. Meo M and Zumpano G. On the optimal sensor placement techniques for a bridge

structure. *Engineering Structures*, 27:1488-97, 2005.
7. Li DS and Li HN and Fritzen CP. The connection between effective independence and modal kinetic energy methods for sensor placement. *Journal of Sound and Vibration*, 305:945-955, 2007.
8. Celep Z. and Kumbasar N. *Earthquake engineering and earthquake resistant design of structures (in Turkish)*. Beta Publishing, Turkey, 2004.
9. Celep. Z. *Reinforced Concrete Structures (in Turkish)*. Beta Publishing, Turkey, 2009.
10. The language of technical computing MATLAB. Available at: http://www.mathworks.com, version 7.10.246, release 14.0, the mathworks. 2005.
11. Imamovic N. *Model validation of large finite element model using test data*. PhD thesis, Imperial College, London, UK, 1998.
12. Doebling SW. *Measurement of structural flexibility matrices for experiments with incomplete reciprocity*. PhD thesis, Colorado University, http://sdel.colorado.edu/Publications/1995/Theses/Doebling-PhD.pdf, USA, 1996.
13. Kim H.B. and Park Y.S. Sensor placement guide for structural joint stiffness model improvement. *Mechanical System and Signal Processing*, 11(5):651-72, 1997.
14. Kammer DC. Sensor set expansion for modal vibration testing. *Mechanical systems and signal processing*, 19(4):700-716, 2005.
15. Kammer D.C. and Tinker M.L. Optimal placement of triaxial accelerometers for modal vibration tests. *Mechanical Systems and Signal Processing*, 18:29-41, 2004.
16. Middleton D. *An introduction to statistical communication theory*. McGraw-Hill, New York, USA, 1960.
17. Allemang R. J. and Brown D. L. A correlation coefficient for modal vector analysis. In *Proceedings of IMAC I: 1st International Modal Analysis Conference*, pages 110-116, Orlando, Florida, 1982.
18. Website of the instrumented building. Available at: www.erenkoy.k12.tr/. 2007.
19. Worden K and Burrows AP, Optimal sensor placement for fault detection. *Engineering Structures,* 23:885-901, 2001.

6. APPENDIX: SSE Technique- Case I: The initial node set renders target mode shapes linearly independent.

In this situation, the measure of triaxial EFI used to add a sensor is chosen as:

$$EfI3_i^+ = \frac{det(Q^{+3i}) - det(Q_o)}{det(Q_o)} \tag{8}$$

where Q_o is the FIM that corresponds to the initially selected set of triaxes as:

$$Q_o = \phi_{so}^T \phi_{so} \tag{9}$$

ϕ_{so} is the target mode partition matrix that corresponds to the initially selected set of triaxes. Q^{+3i} is the FIM with the *i*th node added to the initial triax set as:

$$Q^{+3i} = Q_o + \phi_{si}^T \phi_{si} = Q_o[I_k + Q_o^{-1} \phi_{si}^T \phi_{si}] \tag{10}$$

where I_k is a *k*-dimensional identity matrix. This measure represents the fractional amount the determinant of the initial information matrix will increase, if the i th candidate node is added to the initial set.